

# Supplement to the response letter to RC1

## Sinking microplastics in the water column: simulations in the Mediterranean Sea

(os-2020-95)

Rebeca de la Fuente, Gábor Drótos, Emilio Hernández-García, Cristóbal López,  
and Erik van Sebille

### Deviations from a spherical particle shape

We quantitatively assess the impact of deviations from a spherical shape through a correction to the settling velocity  $v_s$ . The simplified MRG equation, Eq. (3) of the main text or Eq. (A.1) of Appendix A, is affected by particle geometry through the drag force and the added mass term; however, accelerations are irrelevant for  $v_s$ , so that the added mass term does not appear in its formulation or in the simple approximation of Eq. (1) of the main text. We will compare values of the settling velocity describing nonspherical and spherical particles with the same density.

Most generally, the settling velocity vector  $\mathbf{v}_s$  can be obtained by balancing the drag force  $\mathbf{F}_{\text{drag}}(\mathbf{v} - \mathbf{u})$  (a function of the difference of the particle and the fluid velocities,  $\mathbf{v}$  and  $\mathbf{u}$ , respectively) with the resultant of gravitational and buoyancy forces:

$$0 = \mathbf{F}_{\text{drag}}(\mathbf{v}_s) + V(\rho_p - \rho_f)\mathbf{g}, \quad (1)$$

where  $V$  is the particle's volume,  $\rho_p$  and  $\rho_f$  are the densities of the particle and the fluid, respectively, and  $\mathbf{g}$  is the gravitational acceleration vector. For a spherical particle with radius  $a$ , the Stokes drag force reads as

$$\mathbf{F}_{\text{drag}}^{(\text{sph})}(\mathbf{v} - \mathbf{u}) = -6\pi\mu(\mathbf{v} - \mathbf{u})a, \quad (2)$$

where  $\mu$  is the dynamical viscosity of the fluid. According to [1, 2], an appropriate approximation for small nonspherical particles is

$$\mathbf{F}_{\text{drag}}^{(\text{non})}(\mathbf{v} - \mathbf{u}) = -6\pi\mu(\mathbf{v} - \mathbf{u})\left(\frac{1}{3}a_n + \frac{2}{3}a_s\right), \quad (3)$$

where  $a_n$  is the radius of the sphere with equivalent area projected on the plane perpendicular to the relative velocity  $\mathbf{v} - \mathbf{u}$ , and  $a_s$  is the radius of the sphere with equivalent total surface. From either of the last two equations, the settling velocity is obtained by substituting  $\mathbf{v} - \mathbf{u} = \mathbf{v}_s$ , and solving Eq. (1) for  $\mathbf{v}_s$ . We denote the magnitudes of the settling velocities obtained from Eq. (2) and Eq. (3) by  $v_s^{(\text{sph})}$  and  $v_s^{(\text{non})}$ , respectively.

To characterize the correction in the settling velocity for a given nonspherical particle (with a given density  $\rho_p$ ) with respect to assuming a spherical shape with a radius  $a$ , we will consider

$$q \equiv \frac{v_s^{(\text{non})}}{v_s^{(\text{sph})}} = \frac{3}{4\pi} \frac{V^{(\text{non})}}{a^2 \left(\frac{1}{3}a_n + \frac{2}{3}a_s\right)}, \quad (4)$$

where  $V^{(\text{non})}$  is the real volume of the given particle. In order to evaluate Eq. (4), one has to specify the shape and the size of the particle, its orientation with respect to its relative velocity, and also how  $a$  is derived from its real size.

Note that it is always possible to define an  $a$  for which  $q = 1$ , i.e., for which there is no correction arising from the deviation from a spherical shape. In this sense, any choice of  $a$  representing a spherical shape, including ours in the manuscript, describes the settling velocity of certain nonspherical particles, the question is just their shape and size, which will mutually depend on each other for a given  $a$ . We will nevertheless proceed by choosing a shape class and defining  $a$  along independent considerations, because we intend to link a given  $a$  to a single particle size as identified during the processing of field observations.

The shape of rigid microplastic particles is not usually described in the literature, but we can see photographs of some examples in, e.g., [3, 4, 5]. For an explorative computation, a reasonable choice seems to be a rectangular cuboid with edges  $A$ ,  $B = \hat{B}A < A$  and  $C = \hat{C}A < B < A$ , where one or both of  $\hat{B}$  and  $\hat{C}$  are less than 1 but greater than, say, 0.1.

Under this assumption, the particle size will correspond to the longest edge,  $A$ , of the cuboid if the size is identified through microscopy as the largest extension (“length”; e.g., [6]); and it may be related more to the middle edge,  $B$ , if one thinks of a sieving technique (e.g., [7]). The naive choice will be  $a = A/2$  and  $a = B/2$  in these two cases.

We can substitute either of these choices of  $a$  in Eq. (4), as well as the appropriate formulae describing the actual cuboid.  $V = ABC$  is unique, and so is  $a_s$ ,

$$a_s = \left( \frac{AB + AC + BC}{2\pi} \right)^{\frac{1}{2}}. \quad (5)$$

However,  $a_n$  depends on the particle’s orientation with respect to the relative velocity. Implications will be discussed when interpreting the results, and we take here all three directions parallel to edges  $A$ ,  $B$  and  $C$  to represent different possibilities. The corresponding expressions for  $a_n$  read as

$$a_{n,X} = \left( \frac{ABC}{\pi X} \right)^{\frac{1}{2}} \quad (6)$$

for  $X = A$ ,  $B$  and  $C$ .

After substituting all these expressions in Eq. (4), we obtain

$$q_X^{(A/2)} = 9\pi^{-\frac{1}{2}} \hat{B}\hat{C} \left[ \left( \frac{\hat{B}\hat{C}}{\hat{X}} \right)^{\frac{1}{2}} + 2^{\frac{1}{2}} \left( \hat{B} + \hat{C} + \hat{B}\hat{C} \right)^{\frac{1}{2}} \right]^{-1}, \quad (7)$$

$$q_X^{(B/2)} = \hat{B}^{-2} q_X^{(A/2)}, \quad (8)$$

where  $X = \hat{X}A$  has been introduced.

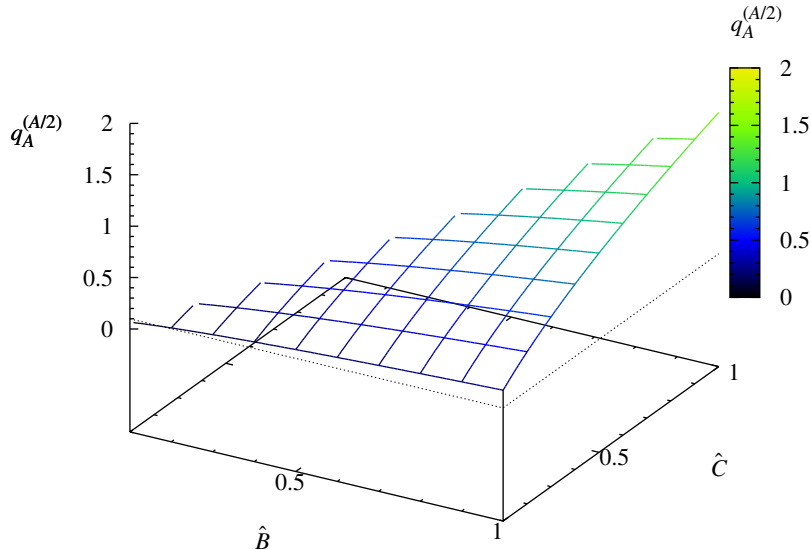


Figure 1:  $q_A^{(A/2)}$  as a function of  $\hat{B}$  and  $\hat{C}$  for  $\hat{B}, \hat{C} \in [0.1, 1]$  with  $\hat{B} > \hat{C}$ . Dotted lines represent  $q_A^{(A/2)} = 0.1$ .

We plot  $q_A^{(A/2)}$  in Fig. 1 as a function of  $\hat{B}$  and  $\hat{C}$  for  $\hat{B}, \hat{C} \in [0.1, 1]$  with  $\hat{B} > \hat{C}$ . Its range extends from 0.07 to 1.5 on this domain, but it drops below 0.1 only for  $\hat{C}$  very close to 0.1 and  $\hat{B}$  below 0.2; i.e., for extremely thin rod-like particles, which do not appear to be common based on photographs. The range of  $q_A^{(B/2)}$  (not shown) on the same domain is between 0.2 and 7, and values above 4 are again restricted to very small  $\hat{C}$  and to  $\hat{B} < 0.3$ . The results are very similar for other choices of  $X$ , deviations beyond 20% with respect to  $X = A$  are only found for small  $\hat{C}$  and do not reach beyond 40% even there.

We have left the question which orientation is relevant open so far. In small-scale isotropic turbulence, which is certainly present in the ocean, nonspherical particles have a preferential alignment with certain characteristics of the flow but undergo rotation [8]. This is why we have chosen to simply cover three perpendicular orientations in our analysis, and have found that differences that may arise from changes in the orientation are minor in most of the domain describing shapes. The only relevant exception is small  $\hat{C}$  with  $\hat{B} \approx 1$ . This regime may characterize paint flakes [3, 5], but the relative difference remains below 40% even there.

Even though the real advection of the particles will become more complicated as a result of the ever-changing orientation and may thus be beyond the scope of the MRG equation (cf. the discussion in the main text about the settling velocity of irregular particles), we have found that changing orientation introduces minor variations in the value of the settling velocity. Together with the absence of order-of-magnitude corrections that may arise from a nonspherical shape (but comparing shapes under the assumption of the same particle density), this gives quantitative support for the applicability of a spherical shape in Eq. (1) of the main text.

Finally, we briefly comment on the more general Eqs. (3) of the main text and (A.1), in which effects from nonsphericity arise in the inertial term through added mass. Since corrections in added mass with respect to a sphere are of order 1 for all common shapes (see [9] for an overview), we believe that the finding of Appendix A about the negligible importance of inertial effects is not affected by a deviation from sphericity.

## Replacements for Figs. A3, A4 and B1 of the manuscript

See the new figures as Figs. 2, 3 and 4 of this supplement, displayed after the reference list.

## References

- [1] David Leith. Drag on nonspherical objects. *Aerosol Science and Technology*, 6(2):153–161, 1987.
- [2] Gary H. Ganser. A rational approach to drag prediction of spherical and nonspherical particles. *Powder Technology*, 77(2):143 – 152, 1993.
- [3] Young Kyoung Song, Sang Hee Hong, Mi Jang, Jung-Hoon Kang, Oh Youn Kwon, Gi Myung Han, and Won Joon Shim. Large accumulation of micro-sized synthetic polymer particles in the sea surface microlayer. *Environmental Science & Technology*, 48(16):9014–9021, 2014. PMID: 25059595.
- [4] Viola Fischer, Nikolaus O. Elsner, Nils Brenke, Enrico Schwabe, and Angelika Brandt. Plastic pollution of the kuril–kamchatka trench area (nw pacific). *Deep Sea Research Part II: Topical Studies in Oceanography*, 111:399 – 405, 2015. The German-Russian deep-sea expedition KuramBio (Kurile Kamchatka Biodiversity Studies) on board of the RV Sonne in 2012 following the footsteps of the legendary expeditions with RV Vityaz.
- [5] A. Bagaev, A. Mizyuk, L. Khatmullina, I. Isachenko, and I. Chubarenko. Anthropogenic fibres in the baltic sea water column: Field data, laboratory and numerical testing of their motion. *Science of The Total Environment*, 599-600:560 – 571, 2017.
- [6] Andrés Cózar, Marina Sanz-Martín, Elisa Martí, J Ignacio González-Gordillo, Bárbara Ubeda, José Á Gálvez, Xabier Irigoien, and Carlos M Duarte. Plastic accumulation in the Mediterranean Sea. *PLoS One*, 10(4), 2015.
- [7] Giuseppe Suaria, Carlo G Avio, Annabella Mineo, Gwendolyn L Lattin, Marcello G Magaldi, Genuario Belmonte, Charles J Moore, Francesco Regoli, and Stefano Aliani. The mediterranean plastic soup: synthetic polymers in Mediterranean surface waters. *Scientific Reports*, 6:37551, 2016.
- [8] Greg A. Voth and Alfredo Soldati. Anisotropic particles in turbulence. *Annual Review of Fluid Mechanics*, 49(1):249–276, 2017.
- [9] Chapter 8 - vibrations in fluid–structure interaction systems. In Shigehiko Kaneko, Tomomichi Nakamura, Fumio Inada, Minoru Kato, Kunihiko Ishihara, Takashi Nishihara, and Mikael A. Langthjem, editors, *Flow-induced Vibrations (Second Edition)*, pages 359 – 401. Academic Press, Oxford, UK, second edition edition, 2014.

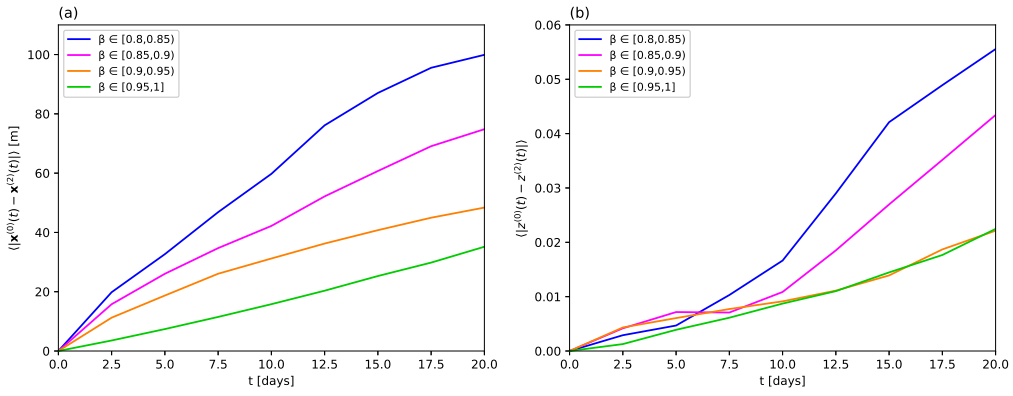


Figure 2: Replacement for Fig. A3 of the manuscript.

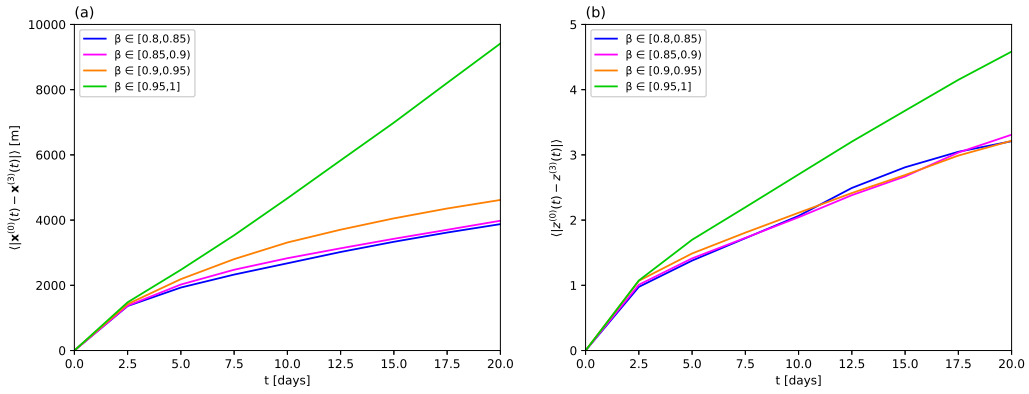


Figure 3: Replacement for Fig. A4 of the manuscript.

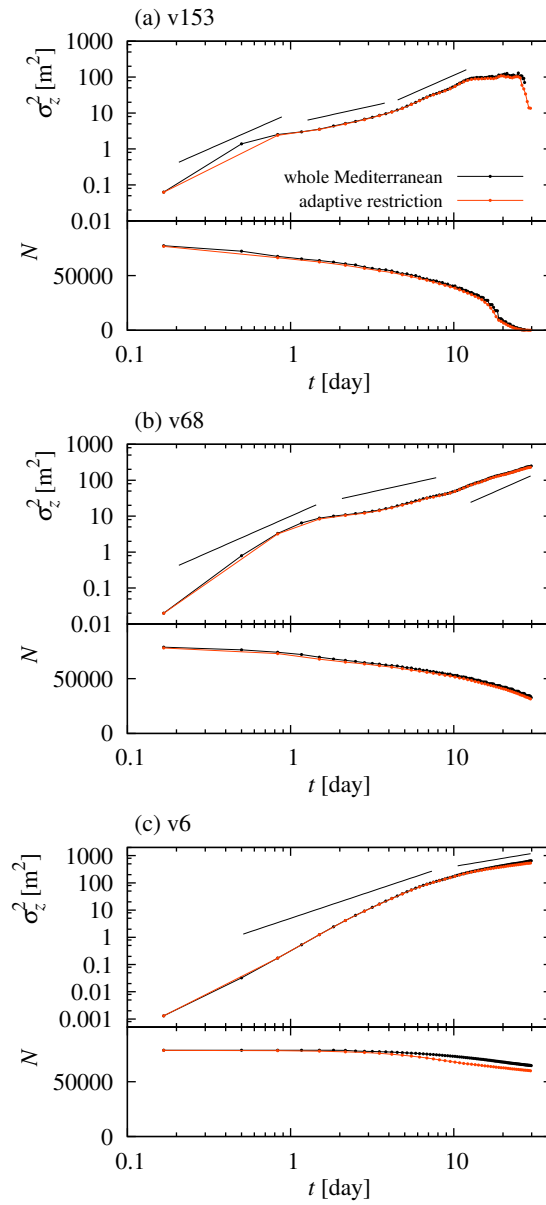


Figure 4: Replacement for Fig. B1 of the manuscript.